

# We are IntechOpen, the world's leading publisher of Open Access books Built by scientists, for scientists

4,800

Open access books available

122,000

International authors and editors

135M

Downloads

Our authors are among the

154

Countries delivered to

TOP 1%

most cited scientists

12.2%

Contributors from top 500 universities



WEB OF SCIENCE™

Selection of our books indexed in the Book Citation Index  
in Web of Science™ Core Collection (BKCI)

Interested in publishing with us?  
Contact [book.department@intechopen.com](mailto:book.department@intechopen.com)

Numbers displayed above are based on latest data collected.  
For more information visit [www.intechopen.com](http://www.intechopen.com)



# Multi-Scale Deconvolution of Mass Spectrometry Signals

M'hamed Boulakroune<sup>1</sup> and Djamel Benatia<sup>2</sup>

<sup>1</sup>*Electrical Engineer Department,*

*Faculty of Sciences and Technology, Kasdi Merbah Ouargla University, Ouargla*

<sup>2</sup>*Electronics Department,*

*Faculty of Engineer Sciences, Université Hadj-Lakhdar de Batna, Batna*

*Algeria*

## 1. Introduction

It has become more important to measure accurate depth profiles in developing more advanced devices. To this aim, Depth profiling in secondary ion mass spectrometry (SIMS) has been extensively used as an informative technique in the semiconductor and electronic devices fields due to its high sensitivity, quantification accuracy and depth resolution (Fujiyama et al, 2011; Seki et al, 2011). However, the depth resolution in SIMS analysis is still limited to provide reliable and precise information in very thin structures such as delta layers, abrupt interfaces, etc. By optimization of the experimental conditions, the depth resolution can be enhanced. In particular, lowering the primary energy seems to be a good solution, but this increases the measurement time and leads to other limitations, owing to the wrong focalization of primary ion beam, such as roughness in the crater bottom, not flat crater, etc. Therefore, the depth resolution remains so far to its perfect limit. It is only by numerical processing like deconvolution that the depth resolution can be improved beyond its experimental limits.

For the past several years, different approaches of deconvolution have been proposed taking into account the different physical phenomena that limit depth resolution, such as collisional mixing, roughness, and segregation (Makarov, 1999; Gautier et al, 1998; Fares et al, 2006; Dowsett et al, 1994; Mancina et al, 2000; Shao et al, 2004; Collins et al, 1992; Allen et al, 1993; Fearn et al, 2005). However, most problems encountered in these deconvolution methods are due to the noise content in the measured profiles. This instrumental phenomenon, which cannot be eliminated by the improvement of operating conditions, strongly influences the depth resolution and therefore the quality of the deconvoluted profiles.

The deconvolution of depth profiling data in SIMS analysis amounts to the solution of an appropriate ill-posed problem in that any random noise in data leads to no unique and no stable solution (oscillatory signal with negative components, which are physically not acceptable in SIMS analysis). Thus, the results must be regularized (Tikhonov, 1963; Barakat et al, 1997; Prost et al, 1984; Burdeau et al, 2000; Herzel et al, 1995; Iqbal, 2003; Varah, 1983;

Essah, 1988; Brianzi, 1994; Stone, 1974; Connolly et al, 1998; Berger et al, 1999; Thompson et al, 1991; Fischer et al, 1998). To this end, the solution is superimposed with certain limitations by introducing some additional limitative operators, whose shape is chosen depending on the formalism used for the solution of the ill-posed problem, into a goal function; usually the goal function is the mismatch between the convoluted solution and the initial data (Makarov, 1999). Indeed, different forms of limitative operator have been used. For example, Collins and Dowssett (Collins et al, 1992) and Allen and Dowssett (Allen et al, 1993) have used the entropy function as a limitative operator. Based on the Tikhonov-Miller regularization, Gautier et al (Gautier et al, 1998) have used a limitative operator that was defined as smoothness of the solution. Mancina et al (Mancina et al, 2000) have introduced *a priori* a pre-deconvoluted signal as a model of solution in an iterative regularized method. Nevertheless, the results of most of these approaches contain artifacts with negative concentrations, which are not physically acceptable. The origin of these artifacts is related to the presence of strong local components of high frequencies in the signal which form part of the noise. To remove the negative components from the deconvoluted profile, some algorithms with non-negativity constraints have been proposed (Makarov, 1999; Gautier et al, 1998; Gautier et al, 1998; Prost et al, 1984). These methods, which constrain the data to be positive everywhere, are sensitive to noise, i.e., a little perturbation in the data can lead to a great difference in the deconvoluted solution. A truncation of the negative data is an arbitrary operation and it is not acceptable, since it results in an artificially steep slope and can lead to the adoption of subjective criteria for profile assessment (Herzel et al, 1995). Moreover, noise in the data increases the distance between the real signal and its estimate, therefore *a priori* constraint is not enough, and a free-oscillation deconvolution is necessary.

To overcome these limits, it is important to adopt a powerful deconvolution that leads to a smoothed and stable solution without application of any kind of constraints. In this context, multiscale deconvolution (MD), which is never used to recover SIMS profiles, may be the most appropriate technique.

The MD provides a local smoothness property with a high smoothness level in unstructured regions of the spectrum where only background occurs and a low smoothness level where structures arise (Fischer et al, 1998). Based on wavelet transform, the MD seems to be a good solution that can yield information about the location of certain frequencies in the profile on different frequency scales. Therefore, high frequencies, which are related to noise, can be localized and controlled at different levels of wavelet decomposition. The multiscale description of signals has facilitated the development of wavelet theory and its application to numerous fields (Averbuch & Zheludev, 2009; Charles et al, 2004; Fan & Koo, 2002; Neelamani et al, 2004; Zheludev, 1999; Rashed et al, 2007; Garcia-Talavera et al, 2003; Starck et al, 2003; Jammal et al, 2004; Rucka et al, 2006). This chapter is intended to explore capabilities of wavelets for the deconvolution framework. The proposed idea is to introduce a wavelet-based methodology in the Tikhonov-Miller regularization scheme and shrinking the wavelet coefficients of the blurred and the estimated solution at each resolution level allow a local adaptation of limitative operator in the quadratic Tikhonov-Miller regularization. This leads to compensation for high frequencies which are related to noise. As a result, the oscillations which appear in classical regularization methods can be removed. This leads to a smoothed and stable solution.

This work is based on SIMS data, for which reason the results presented here are largely restricted to the conditions of SIMS analysis. The main objective of this work is to show that the MD gives much better deconvolution results than those obtained using monoresolution regularization methods. In particular, the results obtained are compared to those achieved using a regularized monoresolution deconvolution, which is Tikhonov-Miller regularization with a pre-deconvoluted signal as a model of the solution, denoted as TMMS (Mancina et al, 2000).

## 2. Deconvolution procedure

### 2.1 Background

Depth profiling in SIMS analysis is mathematically described by the convolution integral which is governed by the depth resolution function (DRF),  $h(z)$ . If the integral over  $h(z)$  is normalized to unity, then the measured (convolved) signal is given by the well-known convolution integral

$$y(z) = \int_{-\infty}^{+\infty} h(z - z') x(z') dz' + b(z), \quad (1)$$

where  $x(z)$  is the compositional depth distribution function and  $b(z)$  is the additive noise.

This work deals with the deconvolution of depth profiling SIMS data. Therefore, it is important for further consideration to know the shape of the DRF that is typical of SIMS profiles. We have chosen to describe the DRF analytically in a form initially proposed by Dowsett et al (Dowsett et al, 1994), which is constituted by the convolution of double exponential functions with a Gaussian function. This DRF can be described by three parameters:  $\lambda_u$  (the rising exponential decay),  $\sigma_g$  (the standard deviation of the Gaussian function), and  $\lambda_d$  (the falling exponential decay). The latter characterizes the residual mixing effect, which is considered to be the main mechanism responsible for the degradation of the depth resolution (Boulakroune et al, 2007; Yang et al, 2006). For any possible values of these parameters, the DRF is normalized to unity. The consequences of the fact that the resolution function can be represented in the form of a convolution have been described elsewhere (Gautier et al, 1998; Dowsett et al, 1994; Collins et al, 1992; Allen et al, 1993).

For a discrete system, eq. (1) can be written as

$$y_k = \sum_{i=0}^{N-1} x_i h_{k-i} + b_k, \quad k=0, \dots, 2N-2, \quad (2)$$

where  $N$  is the number of samples of vectors  $h$ ,  $x$ . Equation (2) can be rewritten as

$$y = Hx + b, \quad (3)$$

where  $H$  is a matrix built from  $h(z)$ . In the case of a linear and shift-invariant system,  $H$  is a convolution operator (circular Toeplitz matrix). This means that the multiplication of  $H$  with the vector  $x$  leads numerically to the same operation as the analytical convolution of  $h(z)$  with  $x(z)$ .

The problem of the recovery of the actual function  $x$  from eq. (3) is an ill-posed problem in the sense of Hadamard. (Varah, 1983) Therefore, it is affected by numerical instability, since  $y$  contains experimental noise. The term incorrectly posed or ill-posed problem means that the solution  $x$  of eq. (3) may not be unique, may not exist, or may not depend continuously on the data. In other words,  $H$  is an ill-conditioned matrix, or/and small variations in the data due to noise result in an unbounded perturbation in the solution.

It is well-known that the function  $H(\nu)$  (the spectrum of the DRF) is a low-pass filter. (Allen, 1993; Barakat, 1997; Berger, 1999; Gautier, 1998) Its components are thus equal or very close to zero for frequencies above a certain cut-off frequency  $\nu_c$ . Components close to  $\nu_c$  are very attenuated by the convolution. Furthermore, in the presence of an ill-posed problem, some components below  $\nu_c$  can be very small, almost null (see Fig. 1). In this case, the inversion of the convolution equation fails for these components, or leads to a very unstable solution.

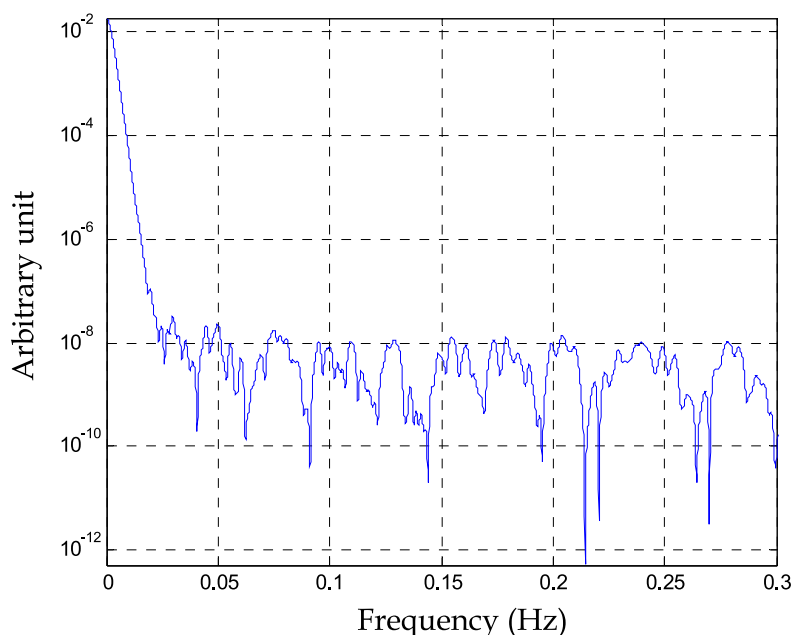


Fig. 1. DFT of the depth resolution function; DRF measured at 8.5 keV/O<sub>2</sub><sup>+</sup>.

To solve an ill-posed problem, it is mandatory to find a solution so that the small components of  $H(\nu)$  do not hinder the deconvolution process, i.e., to stabilize the solution. Moreover, the resolution of an ill-posed problem in the presence of noise leads to an infinite number of solutions, among which it is necessary to choose the unique solution that fits the problem we are trying to solve.

Therefore, in order to solve this problem, a regularization method must be included. This means that the original problem is replaced by an approximate one whose solutions are significantly less sensitive to errors in the data,  $y$ . Several regularization methods have been discussed in refs. (Iqbal, 2003; Varah, 1983; Essah, 1988; Brianzi, 1994; Stone, 1974; Connolly et al, 1998; Berger et al, 1999; Thompson et al, 1991). All of these methods are based on the incorporation of a priori knowledge into the restoration process to achieve stability of the solution.

The basic underlying idea in the regularization approaches is formulated as an optimization problem whose general expression is

$$L\{\tilde{x}(\alpha, y)\} = \{L_1(x, \tilde{x}_0) + \alpha L_2(x, \tilde{x}_\infty)\}_{x \in X} \quad (4)$$

where  $L_1$  is a quadratic distance, which provides a maximum fidelity to the data;  $\tilde{x}_0$  is the least squares solution, consistent with the data;  $L_2$  is a stabilizing function, which measures the distance between  $x$  and an extreme solution  $\tilde{x}_\infty$  corresponding to an a priori ultra-smooth solution. The restoration methods, cited in references (Iqbal, 2003; Varah, 1983; Essah, 1988; Brianzi, 1994; Stone, 1974; Connolly et al, 1998; Berger et al, 1999; Thompson et al, 1991), differ from each other in the choice of the distance  $L_2$ . The choice leads either to a deterministic or a stochastic regularization.  $\alpha$  is the regularization parameter which controls the trade-off between stability (fidelity to the a priori) and accuracy of the solution (fidelity to the data).  $X$  represents the set of possible solutions.

## 2.2 Tikhonov-Miller regularization

As shown in the previous section, the regularization is achieved through a compromise between choosing one solution in the set of solutions that lead to a reconstructed signal close to the measured data (fidelity to the data), and in the set of stable solutions that conform to some prior knowledge of the original signal (fidelity to the a priori). This means that the solution is considered to be close to the data if the reconstruction signal  $Hx$  is close to the measured one  $y$ , i.e., if  $\|y - Hx\|^2$  is reasonably small. Thus, the first task of the deconvolution procedure is to minimize the quadratic distance between  $y$  and  $Hx$ . Unfortunately, solutions that lead to very small values of  $\|y - Hx\|^2$  oscillate and are therefore unacceptable. In order to get a stable solution, one must choose another criterion that checks whether the solution is consistent with the solution of the deconvolution problem: it must be physically acceptable, i.e., a smoothed solution. The smoothness of the solution can be described by its regularity  $r^2$ , defined as

$$\|Dx\|^2 \leq r^2, \quad (5)$$

where  $D$  is a stabilizing operator. The choice of  $D$  is based on the processing context and some a priori knowledge about the original signal.  $D$  is usually designed to smooth the estimated signal, and then a gradient or a discrete Laplacian is conventionally chosen. In this work, the filter used is a discrete Laplacian:  $[1 \ -2 \ 1]$ , its spectrum is a high-pass filter (Gautier et al, 1998; Mancina et al, 2000; Burdeau et al, 2000). This results in the minimization of the quadratic functional proposed by Tikhonov

$$\tilde{x} = \operatorname{argmin} [\|y - H\tilde{x}\|^2 + \alpha(\|D\tilde{x}\|^2 - r^2)], \quad (6)$$

where “argmin” denotes the argument that minimizes the expression between the brackets. Perfect fidelity to the data is achieved for  $\alpha = 0$ , whereas perfect matching with a priori knowledge is achieved for  $\alpha = \infty$ . Therefore, it is necessary to find the optimum  $\alpha$  and, hence, a smoothing factor at which the solution of eq. (6) is well-stabilized and still close to a



real distribution. This regularization parameter  $\alpha$  can be estimated by a variety of techniques (Iqbal, 2003; Varah, 1983; Essah, 1988; Brianzi, 1994; Stone, 1974; Connolly et al, 1998; Berger et al, 1999; Thompson et al, 1991). In a simulation where the regularity of the solution is known,  $\alpha = b^2/r^2$ , where  $b^2$  is an upper bound for the total power of the noise. Unfortunately, in the real case, there is no knowledge of the regularity of the real profile, but it can be estimated by means of the generalized cross-validation (Thompson et al, 1991) which applies well to Gaussian white noise. The regularized solution takes the following form:

$$\tilde{x} = (H^T H + \alpha D^T D)^{-1} H^T y = (H^+)^{-1} H^T y, \quad (7)$$

where  $H^+ = H^T H + \alpha D^T D$ .

The matrix  $H$  characterizing the deconvolution process before regularization is replaced by the generalized matrix  $H^+ = (H^T H + \alpha D^T D)$ , which is more conditioned. That step is carried out by the modification of the eigenvalues of  $H$ ; thus the system becomes more stable. Figure 2 shows the spectra of the DRF ( $H$ ), the filter  $D$  and the generalized matrix  $H^+$ .

The choice of the regularization operator  $D$  should not constitute a difficulty since the rule on the modification of the eigenvalues is respected. The most appropriate choice to be determined for the reconstruction quality is that of the regularization parameter  $\alpha$ . Indeed, a poor estimation of this parameter leads to worse conditioning of the matrix  $H$ , and as a consequence, the solution is degenerated.

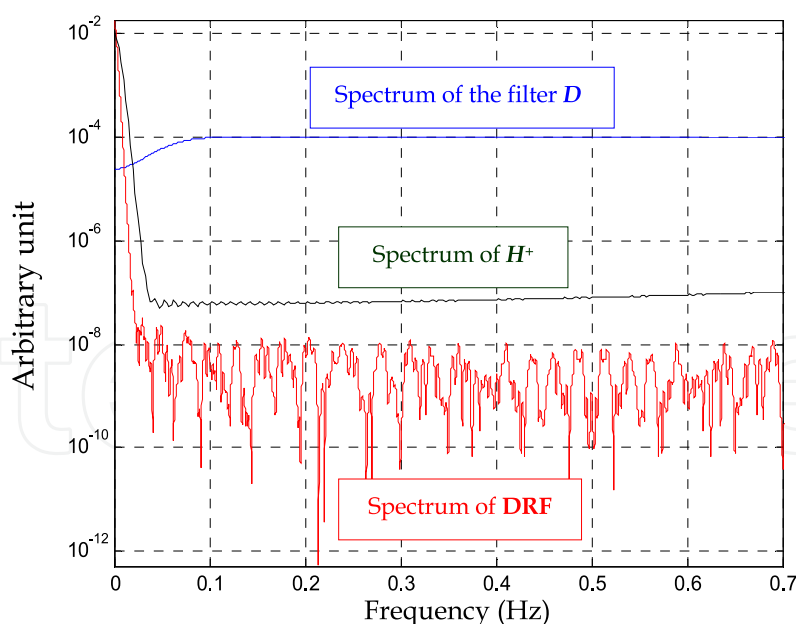


Fig. 2. Spectra of DRF ( $H$ ), filter  $D$ , and the generalized matrix  $H^+$ . Here the regularization parameter  $\alpha$  is overestimated, which leads to a well-conditioned  $H^+$ .

Actually, the regularization can guarantee unicity and stability of the solution but cannot lead to a very satisfactory result. The quantity of information brought is not sufficient to

obtain a solution close to the ideal solution because this regularization provides global properties of the signal. Barakat et al (Barakat et al, 1997) have proposed a method based on Tikhonov regularization combined with an a priori model of the solution. The idea of such a model is to introduce local characteristics of the signal. This model may contain discontinuities whose locations and amplitudes are imposed. The new functional to be minimized with respect to  $x$  is defined as follows:

$$L = \|y - H\tilde{x}\|^2 + \alpha \|D(\tilde{x} - x_{\text{mod}})\|^2, \quad (8)$$

where  $x_{\text{mod}}$  is an a priori model of the solution. The solution of eq. (8) is given by:

$$\tilde{x} = (H^T H + \alpha D^T D)^{-1} (H^T y + \alpha D^T D x_{\text{mod}}). \quad (9)$$

The strategy developed in Barakat's algorithm is useful if the a priori information is quite precise and the quality of solution depends on the accuracy of a priori information.

Mancina et al (Mancina et al, 2000) proposed to reiterate the algorithm of Barakat (Barakat et al, 1997) and to use a pre-deconvoluted signal as model of the solution (an intermediate solution between the ideal solution, i.e., the input signal, and the measured one) with sufficient regularization. The mathematical formulation of the Mancina approach in Fourier space is as follows:

$$\begin{cases} \hat{X}_{n+1} = \frac{H^* Y + \alpha |D|^2 X_{\text{mod}_n}}{|H|^2 + \alpha |D|^2} \\ X_{\text{mod}_n} = TF[\hat{C}\hat{x}_n] \\ \hat{x}_n = TF^{-1}[\hat{X}_n] \\ X_{\text{mod}_0} = 0 \end{cases}, \quad (10)$$

where  $H^*$  is the conjugate of  $H$ , and  $C$  represents the constraint operator which must be applied in the time domain after an inverse Fourier transformation.

Actually, in most of the classical monoresolution deconvolution methods, the results obtained are oscillatory Makarov, 1999; Gautier et al, 1998; Fares et al, 2006; Dowsett et al, 1994; Mancina et al, 2000; Yang et al, 2006; Shao et al, 2004. The generated artifacts are mainly due to the strong presence of high-frequency components which are not compensated by the regularization parameter  $\alpha$  associated with the regularization operator  $D$ , since, in these methods, this parameter is applied in a global manner to all the frequency bands of the signal. This leads to the treatment of the low frequencies, which contain the useful signal, as opposed to the high frequencies, which are mainly noise. Thus, at  $\alpha = 0$ , eq. (7) corresponds to the minimum of  $\arg\min$  [eq. (6)] without smoothing of  $x$ . The corresponding solution is applicable only in the perfect case, i.e., if there are no errors or noise in the experimental distribution  $y$ . Real  $y$  always contains errors, and minimization of eq. (6) using  $\alpha = 0$  produces strong fluctuations of the solution (a parameter  $\alpha$  that is too weak leads to a solution dominated by the noise within the observed data). With an increase of  $\alpha$ , the role of the second term in eq. (6) increases, and the solution stabilizes and becomes increasingly smooth. However, if  $\alpha$  is too large,



surplus smoothing may noticeably broaden the solution and conceal its important features (a parameter  $\alpha$  that is too high leads to a solution that is not very sensitive to noise, but it is very far from the measured data). It is therefore necessary to find the optimum  $\alpha$  and, hence, a smoothing factor at which the solution to problem (6) is well-stabilized but still close to the real distribution. Moreover, in the iterative algorithms, if the regularization parameter is not well calculated, the oscillations created at iteration  $n$  are amplified at iteration  $n + 1$ , which degenerates the final solution. The value of  $\alpha$ , the regularization parameter associated with  $D$ , is very important in the regularization process, and its value determines the quality of the final solution. This can easily be understood if one analyzes the generalized matrix  $H^+$ . As  $\alpha$  increases, the matrix  $(H^+)^{-1}$  tends toward a diagonal matrix, while the vector  $H^T y$ , which is broadened in comparison to the initial data vector  $y$  due to the multiplication by the transposed distortion matrix, remains unchanged. As a result, with an increase of  $\alpha$ , the shape of the solution tends to  $H^T y$ , i.e., to the considerably broadened initial data. Figure 3 shows an example of the evolution of the spectrum of the matrix  $H^+$  for various values of the regularization parameter  $\alpha$ .

According to Fig. 3, the determination of the classical regularization parameter  $\alpha_c$  for the SIMS profile led to a value of  $5.9290 \times 10^{-4}$ . For this value, the spectrum of the generalized matrix  $H^+$  is oscillatory (the matrix is not well-conditioned), leading to an unstable solution. In order to stabilize the system more, Mancina et al (Mancina et al, 2000) proposed multiplying the regularization parameter by a positive factor. The multiplication of this parameter by a factor  $K$  ( $K = 10, 10^2, 10^3$ ) leads to increasingly regularized matrix  $H^+$  (Fig. 2). Nevertheless, this multiplication is arbitrary and it is not based on any physical support

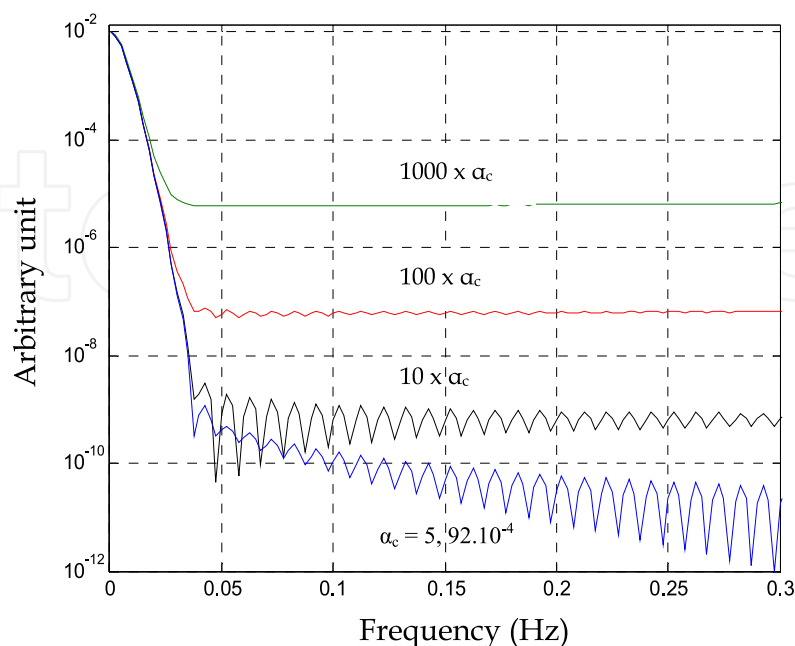


Fig. 3. Evolution of the spectrum of the matrix  $H^+$  according to  $k\alpha_c$  ( $K = 1, 10, 10^2, 10^3$ ).

Since the real distribution that is to be deconvoluted is unknown other than in some special cases, the choice of the optimum  $\alpha$  requires the use of indirect and sometimes non strict and ambiguous criteria. This causes a clear indeterminacy in the choice of  $\alpha$ . One should note that this indeterminacy in ill-posed problems is inherent to any data deconvolution method.

Conventionally, the Tikhonov-Miller approach of searching for the optimum  $\alpha$  uses additional information on the level of noise in the initial data. This is often inconvenient, for example, if the data vary over a wide range, and the statistical noise level changes considerably from point to point depending on signal level.

Generally, the choice of optimum smoothing for deconvolution of an arbitrary set of data requires a special study, and this work only outlines the principle for solving this problem. The example in Fig. 3 shows that the regularization parameter must be accurately determined and locally adapted in the differently treated frequency bands in order to ensure a non aberrant result. This allows the deconvolution of signals previously decomposed by projection onto a wavelet basis.

### 3. Discrete wavelet transform

#### 3.1 Background

Wavelet theory is widely used in many engineering disciplines (Rashed et al, 2007; Garcia-Talavera et al, 2003; Starck et al, 2003; Jammal et al, 2004; Rucka et al, 2006), and it provides a rich source of useful tools for applications in time-scale types of problems. The attention to study of wavelets becomes more attractive when Mallat (Mallat, 1989) established a connection between wavelets and signal processing. Discrete wavelet transform (DWT) is an extremely fast algorithm that transforms data into wavelet coefficients at discrete intervals of time and scale, instead of at all scales. It is based on dyadic scaling and translating, and it is possible if the scale parameter varies only along the dyadic sequence (dyadic scales and positions). It is basically a filtering procedure that separates high and low frequency components of signals with high-pass and low-pass filters by a multiresolution decomposition algorithm (Mallat, 1989). Hence, the DWT is represented by the following equation:

$$W(j, k) = \sum_j \sum_k y(k) 2^{-j/2} \psi(2^{-j}n - k), \quad (11)$$

where  $y$  is discretized heights of the original profile measurements,  $\psi$  is the discrete wavelet coefficients, and  $n$  is the sample number. The translation parameter  $k$  determines the location of the wavelet in the time domain, while the dilatation parameter  $j$  determines the location in the frequency domain as well as the scale or the extent of the space-frequency localization.

The DWT analysis can be performed using a fast, pyramidal algorithm by iteratively applying low-pass and high-pass filters, and subsequent down-sampling by 2 (Mallat, 1989). Each level of the decomposition algorithm then yields to low-frequency components of the

signal (approximations) and high-frequency components (details). This is computed with the following equations:

$$y_{\text{low}}[k] = \sum_n y[n]f[2k-n], \quad (12)$$

$$y_{\text{high}}[k] = \sum_n y[n]g[2k-n], \quad (13)$$

where  $y_{\text{low}}[k]$  and  $y_{\text{high}}[k]$  are the outputs of the low-pass ( $f$ ) and high-pass ( $g$ ) filters, respectively, after down sampling by 2. Due to down-sampling during decomposition, the number of resulting wavelet coefficients at each level is exactly the same as the number of input points for this level. It is sufficient to keep all detail coefficients and the final approximation coefficients (at the roughest level) in order to reconstruct the original data.

The approximation and details at the resolution  $2^{-(j+1)}$  are obtained from the approximation signal at resolution  $2^{-j}$ . In the matrix formalism, eqs. (12) and (13) can be written as

$$y_a^{(j+1)} = F y_a^{(j)}, \quad y_d^{(j+1)} = G y_a^{(j)}, \quad (14)$$

where  $F$  and  $G$  are Toeplitz matrices constructed from the filters  $f$  and  $g$ , respectively.

The reconstruction algorithm involves up-sampling, i.e., inserting zeros between data points, and filtering with dual filters. By carefully choosing filters for the decomposition and reconstruction that are closely related, we can achieve perfect reconstruction of the original signal in the inverse orthogonal wavelet transform (Daubechies, 1990). The reconstructed signal is obtained from eq. (14) by

$$\tilde{y} = \tilde{F} y_a^{(j)} + \tilde{G} y_d^{(j)}, \quad j = 1, \dots, J, \quad (15)$$

where  $\tilde{F}$  and  $\tilde{G}$  are Toeplitz matrices constructed from the reconstruction filters  $\tilde{f}$  and  $\tilde{g}$ , respectively. For a general introduction to discrete wavelet transform and filter banks, the reader is referred to refs. (Mallat, 1989; Daubechies, 1990).

The Mallat algorithm (Mallat, 1989) is a fast linear operation that operates on a data vector whose length is an integer power of two, transforming it into numerically different vectors of the same length. Many wavelet families are available. However, only orthogonal wavelets (such as Haar, Daubichies, Coiflet, and Symmlet wavelets) allow for perfect reconstruction of a signal by inverse discrete wavelet transform, i.e., the inverse transform is simply the transpose of the transform. Indeed, the selection of the most appropriate wavelet is based on the similarity between the derivatives of the signal and the number of wavelet vanishing moments. In practice, wavelets with a higher number of vanishing moments give higher coefficients and more stable performance. In this study, we restrict ourselves to Symlet and Coiflet families; after some experimentation, we chose "Sym4" wavelet with four vanishing moments and "Coif3" wavelet with three vanishing moments. Figure 4 shows the wavelet function, scaling function and the four filters of the wavelets "Sym4" and "Coif3". The decomposition on a wavelet basis (to the level 5) of a SIMS profile containing four delta-layers of boron in silicon to approximation and detail signals is illustrated in Fig. 5.

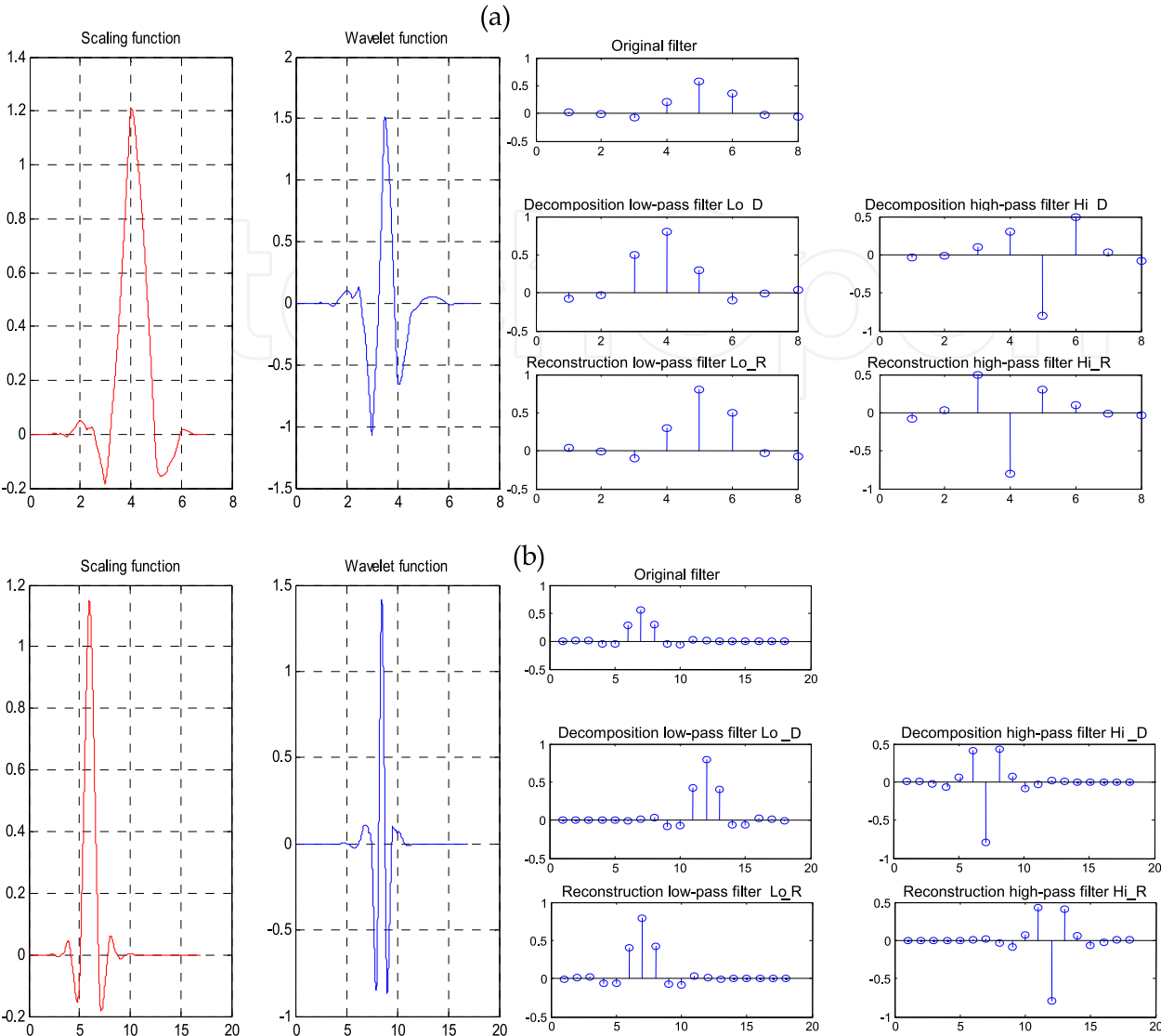


Fig. 4. (a) *Sym4*: scaling function, wavelet function, and the associated filters. (b) *Coif3*: scaling function, wavelet function, and the associated filters.

Due to the compression and dilatation properties of the wavelets in representing a signal, wavelet-based filters can easily follow the sharp edges of the input signal. In other words, they restore any discontinuity in the input signal, or, in terms of the frequency domain interpretation, they pass high frequency components of the input signal. This is a very appealing feature of the wavelet-based methods in many applications, such as finding the location of discontinuities and abrupt changes in a signal. However, this feature may have adverse effects, especially when one wants to get rid of impulsive noise (outliers and gross errors).

We notice that the lower level (high-frequency) wavelet components are similar to a random process, while the higher level (low-frequency) ones are not [Fig. 5(a)]. The noise in SIMS analysis is Gaussian, and one considers that, if there was no signal but the noise alone, the variance of the details would decrease by a factor of 2 at each resolution. Analysis at each level of detail (from small to large) separately on the same signal is shown in Fig. 5(b).

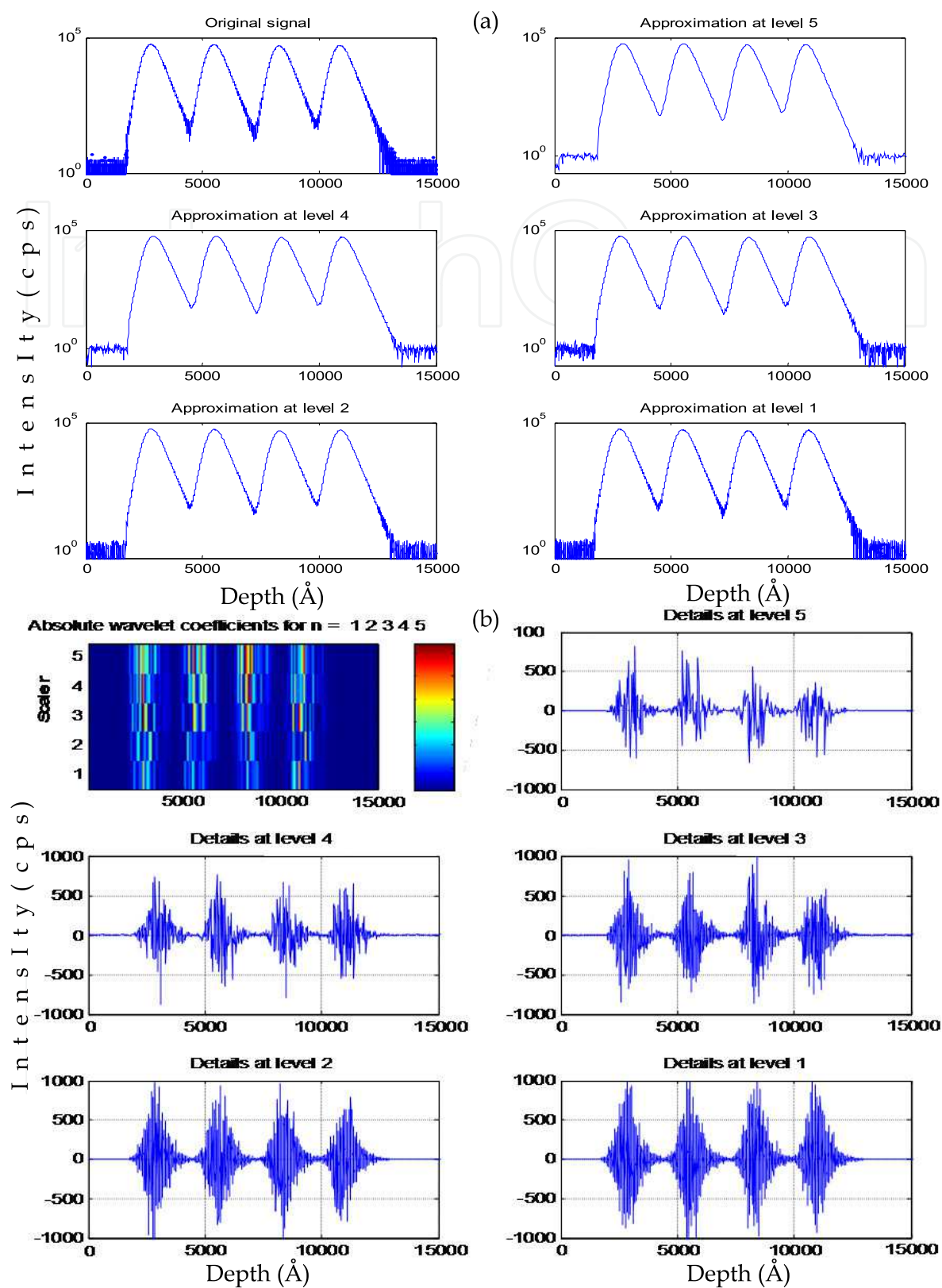


Fig. 5. Wavelet decomposition of SIMS profile measured at 8.5 keV/O<sub>2</sub><sup>+</sup>, 38.1 rad. The wavelet used is *Sym4*; the decomposition level is 5. (a) The original measured profile with the different approximation signals from level 1 to 5. (b) Detail signals from level 1 to 5 with absolute wavelet coefficients



Wavelets have multiscale and local properties that make them very effective in analyzing the class of locally varying signals. Together the locality and multiscale properties enable the wavelet transform to efficiently match signals organized into levels or scales of localized variations. Thus DWT transforms the noisy signal in the wavelet domain, and by denoising we obtain a sparse representation with a few large dominating coefficients (Donoho et al, 1994, 1995). A large part of the wavelet coefficients does not carry significant information [see absolute wavelet coefficients for  $n = 1$  to 5 in Fig. 5(b)]. We select the significant ones by a thresholding procedure, which is addressed in the following section.

### 3.2 Denoising by wavelet coefficients thresholding

Noise is a phenomenon that affects all frequencies. Since the useful signal tends to dominate the low-frequency components, it is expected that the majority of high-frequency components above a certain level are due to noise. In the wavelet decomposition of signals, as has been described, the filter  $h$  is an averaging or smoothing filter, while its mirror  $g$  produces details. With the exclusion of the last remaining smoothed components, all wavelet coefficients in the final decomposition correspond to details. If the absolute value of a detail component is small (or set to zero), the general signal does not change much. Therefore, thresholding the wavelet coefficients is a good way of removing unimportant or undesired (insignificant) details from a signal. Thresholding techniques are successfully used in numerous data-processing domains, since in most cases a small number of wavelet coefficients with large amplitudes preserve most of the information about the original data set.

A basic wavelet-based denoising procedure is described in the following:

- **Decomposition:** Select the level  $N$  and type of wavelets and then determine the coefficients of SIMS signal by DWT. For wavelet denoising, we must decide from many possible selections, such as the type of mother wavelet, the decomposition levels, and the values of thresholds in the next step. In this study, decomposition at level 5 has been used.
- **Thresholding:** Estimating threshold values is based upon the analytical and empirical methods. For each level from 1 to 5, we use the estimated threshold values and set the detail coefficients below the threshold values to zero. Based on knowledge of the wavelet analysis in the data set, we use objective criteria to determine threshold values. Basically, the choice of mother wavelet appears not to matter much, while the values of thresholds do. Therefore, setting the values of the threshold is a crucial topic. According to the analysis described, we set threshold values based on the properties of SIMS data sets.
- **Reconstruction:** We reconstruct the denoised signal using the original approximation coefficients of level  $N$  and the modified detail coefficients of levels from 1 to  $N$  by the inverse DWT.

Wavelet denoising methods generally use two different approaches: hard thresholding and soft thresholding. The hard thresholding philosophy is simply to cut all the wavelet coefficients below a certain threshold to zero. However, soft thresholding reduces the value (referred to as “shrinkage”) of wavelet coefficients towards zero if they are below a certain



value. For a certain wavelet coefficient  $k$  on scale  $j$ , the thresholded details coefficients are given by

$$\hat{y}_d(k) = \text{sign}(|y(k)| - \lambda), \quad (16)$$

where the function “sign” returns the sign of the wavelet coefficient, and  $\lambda$  is the threshold value. In the case of Gaussian white noise (which is the kind of noise in SIMS analysis), Donoho and Johnstone (Donoho et al, 1994, 1995) modeled this threshold by

$$\lambda = \sigma \sqrt{2 \log(N)}, \quad (17)$$

where  $N$  is the number of the observed data points, and  $\sigma$  is the standard deviation of noise. This standard deviation, in the case of white and Gaussian noise, is estimated by

$$\hat{\sigma} = \text{median}(|cd^{(1)}(k)|) / 0.6754, \quad (18)$$

where  $\text{median}(cd^{(1)}(k))$  is the median value of detail coefficients at the first level of decomposition which can be attributed to noise. After thresholding, the reconstructed signal of eq. (15) becomes:

$$\tilde{y} = \tilde{F}y_a^{(j)} + \tilde{G}\hat{y}_d^{(j)}, \quad j = 1, \dots, J. \quad (19)$$

By using this process, high-frequency components above a certain threshold can be removed. A raw SIMS profile and corresponding denoised profile are shown in Fig. 6(a). In particular, the figure shows that low-frequency components, which usually represent the main structure of the signal, are separated from high-frequency components. These preliminary results demonstrate the superior capabilities of the wavelet approach to SIMS profiles analysis over traditional techniques.

In the analysis of SIMS data, we find that most wavelet coefficients at high-frequency levels from 1 to 4 [see Fig. 5(b)], can be mostly ignored. However, we must be very cautious when manipulating the low-frequency components to keep as many true coefficients as possible after thresholding. According to the exploratory data analysis in the beginning of this section, we select a threshold value large enough to ignore most of the wavelet coefficients at levels 1-4, which represent the noise signals, especially in the beginning and the end of the profile. The denoising results show the good performance of wavelet application and exploratory data analysis.

The remaining wavelet coefficients after shrinkage are less than one tenth of those of the original SIMS. These thresholded wavelet coefficients [those “stuttered”  $2^n$  times on level  $n$  are concentrated in the zone where the signal is too noisy, see Fig. 6(b)] give us an idea of the remaining details in the approximation (denoised signal) of the original signal, which are higher than the determined threshold (significant details). For example, the estimated threshold of the previous SIMS signal, obtained using soft universal shrinkage [eq. (17)], is  $\lambda = 55.7831$  cps. The estimated level of noise, using eq. (18), gives a signal-to-noise ratio (SNR) = 40.9212 dB.

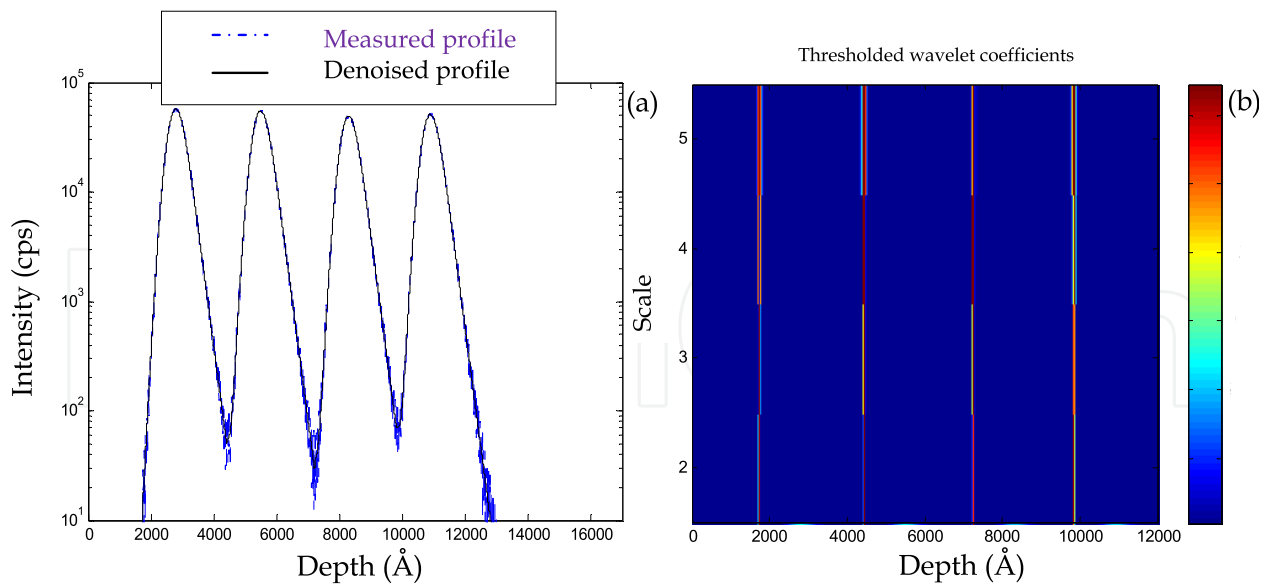


Fig. 6. (a) Original SIMS profile superimposed on the denoised profile. (b) Thresholded wavelet coefficients.

Because the few largest wavelet coefficients preserve almost the entire energy of the signal, shrinkage reduces noise without distorting the signal features. The main results after denoising by wavelet coefficient thresholding are as follows.

- The noise is almost entirely suppressed.
- Sharp features of the original signal remain sharp in the reconstruction.
- It is inferred that progressive wavelet transformations would bring the prediction asymptotically closer towards the true signal.

Finally, we note that the result obtained [Fig. 6(a)] is of both good smoothness and regularity. Thus, we may exploit this advantage in deconvolution procedure without fearing that it will lead to aberrant results.

#### 4. Multiscale deconvolution (MD): The proposed algorithms

##### 4.1 First algorithm: Tikhonov-Miller regularization with a denoisy and deconvoluted signal as model of solution

We have seen in § 2.2 eq. 10 that Mancina (Mancina, 2000) proposed to reiterate the algorithm of Barakat (Barakat et al, 1997) and to use a pre-deconvoluted signal as model of the solution with sufficient regularization. The accuracy of the solution is referred to the accuracy of the model, which suggests a reasonable formulation. It is obvious that a significant lack of precision in the a priori model leads to an error restoration more important than the usual one without the model. Moreover, if the pre-deconvoluted signal is a noisy signal (which is the case for SIMS signals) or contains aberrations, the iterative process worsens these aberrations and the result is an oscillatory signal. For this reason, it is important to remove noise components from the signal (the model of solution). The idea is to introduce a denoisy and deconvoluted signal as model of solution in Barakat's approach, which constitutes our first contribution in this field (Boulakroune, 2008). The first proposed deconvolution scheme is constructed by the following steps:

1. Dyadic wavelet decomposition of the noisy signal at the resolution  $2^{-i}$ .
2. Denoising of this signal by thresholding. One conserves only high-frequency components of details which are above the estimated threshold.
3. Reconstruction of the denoisy signal from the approximations and thresholded details using eq.19.
4. The obtained denoisy signal constitutes the model of solution in iterative Tikhonov-Miller regularization at the first iteration.

The mathematical formulation, in Fourier space, of this algorithm is as follows:

$$\begin{cases} X_{\text{mod}_0} = \tilde{F}y_a^{(j)} + \tilde{G}y_d^{(j)} \\ \hat{X}_{n+1} = \frac{H^*Y + \alpha|D|^2 X_{\text{mod}_n}}{|H|^2 + \alpha|D|^2} \\ X_{\text{mod}_n} = \hat{X}_{n+1} \end{cases} \quad (20)$$

It can be noted that denoising reduces the noise power in data; the regularization parameter should be evaluated by cross-validation in regards of the denoisy signal.

Since the noise is controlled by multiscale transforms, the regularization parameter does not have the same importance as in standard deconvolution methods. Clearly it will be lower than obtained without denoising.

In order to validate the robustness of the proposed algorithm, the results must be compared with those of the previous Tikhonov-Miller regularization algorithms. In particular, we have chosen to compare our results with those obtained by Mancina algorithm (Mancina, 2000).

The results of deconvolution by Mancina's approach (Mancina, 2000) are given in Figs. 7(a) and 7(b). It is obvious by using this algorithm, that the deconvolution has improved the slope and the regularity of the delta layers which are completely separated. Indeed, their shape is symmetrical for all peaks, indicating that the exponential features caused by the SIMS analysis are removed. The full width at half maximum (FWHM) of the deconvoluted delta-layers is equal to 19.5 nm. This can be considered a very good result if one takes into account that the FWHM of the measured profile is approximately 59.7 nm. This corresponds to an improvement in depth resolution by a factor of 3.06. The dynamic range is enhanced by a factor of 2.03 for all peaks.

At both sides of the deconvoluted peaks, oscillations with negative components [Fig. 7(a)] appear under the level of noise where the reliability of the deconvolution process cannot be guaranteed. These artifacts, which have been produced by the deconvolution algorithm, must not be taken for a real concentration distribution. The negative values of these artifacts are not physically accepted for concentration measurements in SIMS analysis. Although a compromise was made between the iteration number and the quality of the deconvoluted peaks, if one increases the iteration number with a relatively weak regularization parameter (obtained by cross validation, it equals  $5.6552 \times 10^{-6}$ ), the number and the level of these oscillations increase more which reinforces the limits of this algorithm. Indeed, these oscillations are directly related to the quantity of noise. Part of this information, in particular in high frequencies, is masked by the noise, and this lack of information is compensated by

the generation of artifacts. With an over estimated value of the regularization parameter, which leads to a more conditioned matrix ( $H^+$ ) (see Fig. 2), one can reduce the number and the amplitude of these oscillations. The solution can be stable and smooth, but this operation is arbitrary and not based on any physical or mathematical support.

By applying the positivity constraint, one reinforces the positivity of the final deconvolution profile. The solution stays in accordance with physical reality, as is illustrated in Fig. 7(b). However, positivizing the signal is an arbitrary operation; it is only to direct the solution so that it becomes positive, without making sure that it is exact. Furthermore, the measured dose (the number of ions counted) must be identical for all signals (original, measured, deconvoluted) except for the noise. This dose must be preserved in the resolution of convolution equation and must take into account the generated negative components. With the application of the positivity constraint, the dose of the deconvoluted and constrained signal is higher than the initial dose. A variation of a few percent cannot be tolerated in the quantification of SIMS profiles. It is important to note that in the case of SIMS analysis, physical coherence is of paramount importance. The deconvoluted profile must be physically acceptable. Thus, it is important to adopt a method whose result is acceptable; otherwise the result obtained may be mathematically correct but have no connection with physical reality.

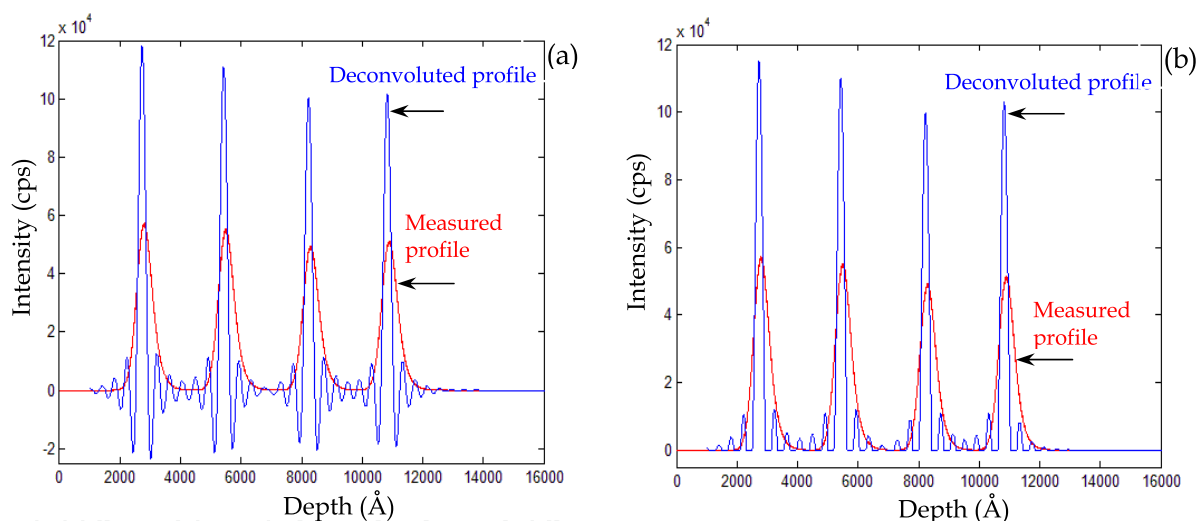


Fig. 7. Results of TMMS algorithm for sample MD4 containing four delta layers of boron in silicon (8.5 keV/ $O_2^+$ , 31.8°);  $\alpha_c = 5.6552 \times 10^{-6}$ ,  $n = 150$  iterations.

(a) Without application of positivity constraint.

(b) With application of positivity constraint.

To completely remove artifacts from the deconvoluted profiles, Gautier et al (Gautier et al, 1997) proposed the application of local confidence level deduced empirically from the reconstruction error in the deconvoluted profiles. The goal of this confidence level is to separate the parts of the signal belonging to the original profile from those generated artificially by the process of deconvolution. According to these authors (Gautier et al, 1997), when the signal falls to the noise level, at which point one cannot be confident in the deconvolution result, one must fix a limiting value of the deconvoluted signal below which one should not take into account the deconvolution result that likely belongs to the original

signal. However, a confidence level that authorizes to take into account certain parts of the signal and eliminates the lower parts in which the signal should not be taken into account any more, does not bring any information about the quality of information. One of the advantages of SIMS analysis is the great dynamic range of the signal, and allowing the deconvoluted signal to be restricted to a dynamic range which does not exceed two decades and thus does not reflect the original signal. The parts filtered by the confidence level can provide precious information about the sample. In ref. (Mancina, 2000), Mancina showed that the artifacts are not always aberrations of the deconvolution; they can be structures with low concentrations. The interpretation of the artifacts must be measured, especially if their amount is not negligible, in which case, one cannot eliminate them from the deconvoluted profiles. Therefore, it is important to find another tool which leads to a solution lacking of any non physical features and without any arbitrary operations.

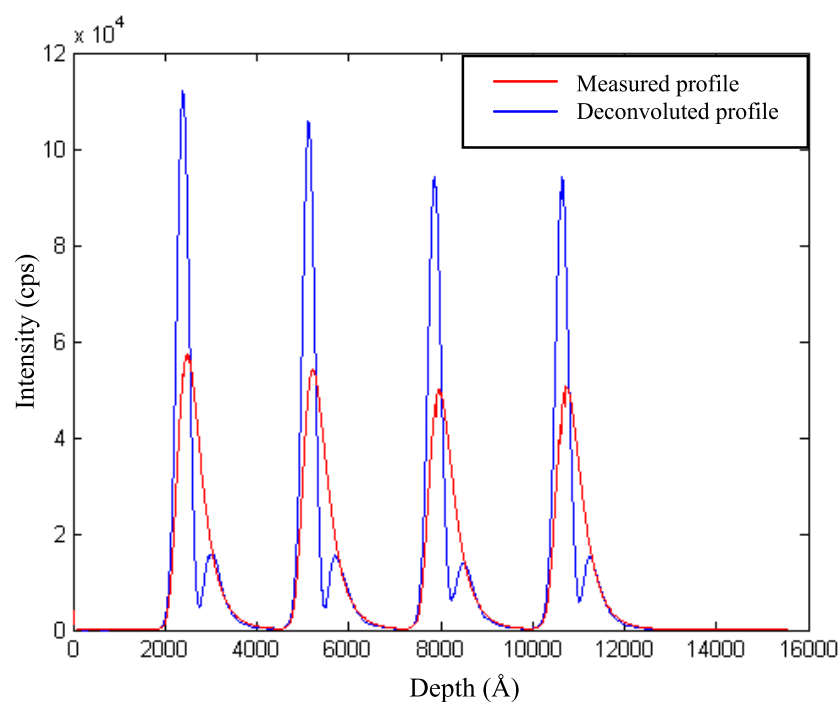


Fig. 8. Result of deconvolution by the first proposed algorithm of SIMS profile containing four delta-layers of boron in silicon (8,5 keV/O<sub>2</sub><sup>+</sup>, 38,1°),  $\alpha = 5,6552 \cdot 10^{-6}$ ,  $n = 250$  iterations. The level of estimated noise, by using (17) et (18), is of SNR = 40,92 dB. The threshold  $\lambda = 55.7831$  counts/s. The used wavelet is Sym4.

By using the first proposed algorithm, the results are quite satisfactory suggesting that this approach is indeed self-consistent, see Fig. 8. A significant improvement in the contrast is observed; the delta layers are more separated. The shape of the results is symmetrical for all layers, indicating that the exponential features (in particular the distorted tail shape observed in the boron profile is due to a significantly larger ion mixing effect) caused by SIMS analysis are removed. The same gains that those obtained by Mancina approach of the depth resolution and maximum of picks (dynamic range) are obtained. It can be noted that the width of measured peaks indicates that the  $\delta$ -layers are not truths deltas - doping, they are close to gaussian more than delta-layers. At the right side of the main deconvoluted peaks some other small peaks appear without any negative component and without



application of positivity constraint any more, which validates this approach. The question for the SIMS user is to know whether these peaks are to be considered as physical features or as deconvolution artifacts. The origin of these *positive* oscillations lies in the strong local concentrations of the high frequencies of noise, and which cannot be correctly restored. It should be noted that these small peaks can be eliminated by the support constraint, but we consider that the application of any kind of constraints is a purely arbitrary operation.

In the classical approaches of the regularization (including our first algorithm) the regularization operator applies in a total way to all bands of the signal. This results in treating low frequencies which contain the useful signal like high frequencies mainly constituted by noise. The result is then an oscillating signal, because the regularization parameter is insufficient to compensate all high frequencies. To overcome these limits, it is important to adopt a powerful deconvolution that leads to a smoothed and stable solution. In this context, multiresolution deconvolution, which is never used to recover SIMS profiles, may be the most appropriate technique.

#### 4.2 Second algorithm: Multiresolution deconvolution

Because of the very abrupt concentration gradients in circuits produced by the microelectronics industry the original SIMS depth profiles are likely to contain some very high frequencies (Gautier et al, 1998). SIMS signals can extend over several decades in a very short range of depth. The intention of any SIMS analyst, as well as of any deconvolution user, is to recover completely all the frequencies lost by the measurement process. Unfortunately, considering again the fact that the resolution function is a low-pass filter, the recovery of high frequencies is always limited, and the recovery of the highest frequencies is definitely impossible, particularly when the profile to be recovered is noisy, which is always the case. It is possible to produce some very high frequencies during the deconvolution process, but there are many chances that these high frequencies are only produced by the high-frequency noise or are created during the inversion of eq. (3) from the very small components of  $H(v)$ . High frequencies in the results of a deconvolution must be regarded suspiciously, except if we are just trying to recover very sharp spikes with no interesting low frequencies. This is definitely not the case for SIMS signals, which contain an appreciable amount of low frequencies, too. Therefore, the purpose of this work is to solve this problem by separating high frequencies and low frequencies in the signal, and then further recovering correctly the high frequencies which are not attributable to noise and which contain useful information. Using multiresolution deconvolution, the final result of the deconvolution should be reasonably smooth. This arises from the observation that, even though the SIMS profiles are likely to contain very high frequencies, which can be thresholded by wavelet shrinkage.

In classical regularization approaches, in order to limit the noise content, one must give a higher bound to the quantity of high frequencies that are likely to be present in the result of the deconvolution [eq. (5)], which might be invalid. However, by this process one limits the quantity of high frequencies, not the quantity of noise. The best solution is to recover correctly the frequencies in different bands of the signal and to find an objective criterion to separate the high frequencies which contain noise from those containing the useful information. Moreover, in these traditional regularized methods (monoresolution



regularized deconvolution), the regularization parameter is applied comprehensively to all signal bands, which results in treating low frequencies which contain the useful signal as high frequencies mainly consisting of noise. The result is then an oscillatory signal, because the regularization parameter is insufficient to compensate high frequencies. Therefore, our idea is to locally adapt the regularization parameter in different frequency bands. This allows us to deconvolute signals previously decomposed by projection onto a wavelet basis.

We have seen in § 3 that the multiscale representation of the signal, or wavelet decomposition allows its associating with an approximation signal at low frequencies (scale coefficients) and a detail signal at high frequencies (wavelet coefficients). Indeed, the approximation signal is very regular (smooth) whereas the detail signal is irregular (rough). This information may be exploited a priori in the deconvolution algorithm. A regular wavelet base will be privileged if one wants to control this regularity, in particular if successive decompositions are used.

It should be noted that the use of a wavelet base with limited support allows preserving a priori knowledge of the signal support in its multiresolution representation. The effectiveness of the constraint of limited support is preserved if the wavelet support is small with respect to that of the signal. In the case of a positive signal, the approximation signal will be positive only if all low-pass filter coefficients are positive. The detail signal always averages to zero; this information can be used like a new soft constraint.

Considering all these advantages, the regularized multiresolution deconvolution can then be performed so that limits of classical monoresolution deconvolution methods are overcome, such as, generating oscillations with negatives components, which limit the depth resolution.

In sharp contrast with the usual multiresolution scheme, it has been established in refs. (Burdeau et al, 2000; Weyrich et al, 1998) that the decimation process is without interest in deconvolution and, in addition, that it incorporates errors in data, if this is the case, then the output of the filters are not decimated.

After wavelet decomposition, the observed noisy data of approximation and details are written under the following mathematical formalism:

$$\begin{aligned} y_a^{(j)} &= H^{(j)} x_a^{(j)} + b_a^{(j)} \\ y_d^{(j)} &= H^{(j)} x_d^{(j)} + b_d^{(j)} \end{aligned} \quad j=1, \dots, J. \quad (21)$$

where  $b_a^{(j)}$  and  $b_d^{(j)}$  represent the approximation and details of the noise at the resolutions  $2^{-j}$  and  $2^{-j}$ , respectively.

We use the Tikhonov regularization method to solve the two parts of eq. (21) separately. The following soft constraints about the solutions  $\tilde{x}_a^{(j)}$  and  $\tilde{x}_d^{(j)}$  are used:

$$\begin{aligned} \|y_a^{(j)} - H^{(j)} \tilde{x}_a^{(j)}\|^2 &\leq \|b_a^{(j)}\|^2 \\ \|y_d^{(j)} - H^{(j)} \tilde{x}_d^{(j)}\|^2 &\leq \|b_d^{(j)}\|^2 \end{aligned} \quad j=1, \dots, J, \quad (22)$$

$$\begin{aligned} \|D_a^{(j)} \tilde{x}_a^{(j)}\| &\leq (r_a^{(j)})^2 \\ \|D_d^{(j)} \tilde{x}_d^{(j)}\| &\leq (r_d^{(j)})^2 \end{aligned} \quad j=1, \dots, J. \quad (23)$$

where  $d_a^{(0)}$  and  $D_d^{(0)}$  are high-pass filters, and  $(r_a^{(0)})^2$ ,  $(r_d^{(0)})^2$  are regularities of approximation and detail solutions at resolutions  $2^{-J}$  and  $2^{-j}$ , respectively.

Following the Miller approach, the constraints are quadratically combined. We then have

$$\begin{aligned} \|y_a^{(j)} - H^{(j)} \tilde{x}_a^{(j)}\|^2 + \frac{\|b_a^{(j)}\|^2}{(r_a^{(j)})^2} \|D_a^{(j)} \tilde{x}_a^{(j)}\|^2 &\leq 2 \|b_a^{(j)}\|^2 \\ \|y_d^{(j)} - H^{(j)} \tilde{x}_d^{(j)}\|^2 + \frac{\|b_d^{(j)}\|^2}{(r_d^{(j)})^2} \|D_d^{(j)} \tilde{x}_d^{(j)}\|^2 &\leq 2 \|b_d^{(j)}\|^2 \end{aligned} \quad j=1, \dots, J. \quad (24)$$

The two deconvolutions are the solutions of the normal equations:

$$\begin{aligned} [(H^{(j)})^T H^{(j)} + \alpha_a^{(j)} (D_a^{(j)})^T D_a^{(j)}] \tilde{x}_a^{(j)} &= (H^{(j)})^T y_a^{(j)} \\ [(H^{(j)})^T H^{(j)} + \alpha_d^{(j)} (D_d^{(j)})^T D_d^{(j)}] \tilde{x}_d^{(j)} &= (H^{(j)})^T y_d^{(j)} \end{aligned} \quad j=1, \dots, J. \quad (25)$$

with

$$\alpha_a^{(j)} = \frac{\|b_a^{(j)}\|^2}{(r_a^{(j)})^2} \quad \text{and} \quad \alpha_d^{(j)} = \frac{\|b_d^{(j)}\|^2}{(r_d^{(j)})^2} \quad j=1, \dots, J. \quad (26)$$

In practice, regularity coefficients  $(r_a^{(0)})^2$ ,  $(r_d^{(0)})^2$  and noise energies  $\|b_a^{(j)}\|^2$ ,  $\|b_d^{(j)}\|^2$  are unknown. Fortunately, these parameters can be estimated using generalized cross-validation (Thompson et al, 1991; Weyrich et al, 1998). The mathematical formalisms of these estimations are:

$$V(\alpha_a^{(j)}) = \frac{\frac{1}{N} \|y_a^{(j)} - H^{(j)} H^{+(j)} H^{T(j)} y_a^{(j)}\|^2}{\left[ \frac{1}{N} \text{Trace}(I - H^{+(j)}) \right]^2}, \quad V(\alpha_d^{(j)}) = \frac{\frac{1}{N} \|y_d^{(j)} - H^{(j)} H^{+(j)} H^{T(j)} y_d^{(j)}\|^2}{\left[ \frac{1}{N} \text{Trace}(I - H^{+(j)}) \right]^2} \quad (27)$$

To solve eq. (24), we must calculate the reverse of the matrices:

$$\begin{aligned} H_a^+ &= (H^{(j)})^T H^{(j)} + \alpha_a^{(j)} (D_a^{(j)})^T D_a^{(j)} \\ H_d^+ &= (H^{(j)})^T H^{(j)} + \alpha_d^{(j)} (D_d^{(j)})^T D_d^{(j)} \end{aligned} \quad j=1, \dots, J. \quad (28)$$

The quality of the solutions  $\tilde{x}_a^{(j)}$  and  $\tilde{x}_d^{(j)}$  depends on the conditioning of the matrices  $H_a^+$  and  $H_d^+$ .

The operators  $D_a^{(0)}$  and  $D_d^{(0)}$  are selected with important eigenvalues when singular values of  $H^{(0)}$  and  $H^{(0)}$  are rather weak. Indeed, the choice of the regularization operators is conducted

based on the singular values of  $H^{(j)}$  and  $H^{(i)}$  but not by the considered frequency-band, because it is not useful to choose an operator for each frequency band. We construct  $D_a^{(j)}$  and  $D_d^{(i)}$  from the same pulse response  $d(n)$ ; this operator is denoted as  $D^{(i)}$  at resolution  $2^j$ .

It is important to note that in a multiresolution scheme up to the resolution  $2^J$ , the different filters responses of decomposition and reconstruction should be interpolated by  $2^{j-1}-1$  zeros at the resolution  $2^j$  in order to contract the filter bandwidth by a factor  $2^{j-1}-1$ . Each matrix should have a size in accordance with the size of the filtered vector that depends on the resolution level.

The different steps in the multiresolution deconvolution algorithm are as follows (Boulakroune, 2009).

1. Dyadic wavelet decomposition of the noisy signal up to the resolution  $2^j$  ( $j = 1, 2, \dots$ ).
2. Denoising of this signal by thresholding. One conserves only high-frequency components of details which are above the estimated threshold. One uses generalized cross-validation for threshold parameter evaluation without prior knowledge of the noise variance. (Weyrich, 1998) It can be noted that the wavelet should be orthogonal, therefore the noise in the approximation and detail remains white and Gaussian if it is, in the blurred signal, white and Gaussian.
3. Solving the two Tikhonov-Miller normal [eq. (22)] at each resolution level.
4. Denoising of the wavelet-decomposed solution of the deconvolution problem by thresholding.
5. Dyadic wavelet undecimated reconstruction of the restored signal up to the full resolution.

By using multiresolution deconvolution, the results are quite satisfactory, suggesting that this approach is indeed self-consistent [Figs. 9(a) and 9(b)]. A significant improvement in contrast is observed; the delta layers are more separated. The shape of the results is symmetrical for all layers, indicating that the exponential features caused by SIMS analysis are removed.

The different regularization parameters obtained using the generalized cross validation [eq. (27)] at different levels necessary for a well regularized system are  $\alpha_a^{(1)} = 3.34789 \times 10^{-4}$ ,  $\alpha_a^{(2)} = 6.7835 \times 10^{-4}$ ,  $\alpha_a^{(3)} = 0.0013$ ,  $\alpha_a^{(4)} = 0.0026$ ,  $\alpha_a^{(5)} = 0.0048$ ,  $\alpha_d^{(1)} = 1.1012$ ,  $\alpha_d^{(2)} = 2.3287$ ,  $\alpha_d^{(3)} = 4.0211$ ,  $\alpha_d^{(4)} = 9.1654$ ,  $\alpha_d^{(5)} = 16.0773$ . The classical regularization parameter is equal to  $6.6552 \times 10^{-5}$ .

The approximation regularization parameter increases proportionally with the decomposition level. This behavior is explained by the decrease of the local regularity of the signal with the scale and inter-scale behavior of wavelet coefficients. The latter determines the visual appearance of the added details information (high frequency contents) in the reconstruction. Therefore, as the degree of accuracy is high, the signal regularity is better; hence, the regularization parameter decreases more.

The detail regularization parameter also decreases according to the decomposition level. This evolution is materialized by the degradation of the precision with the scale, which decreases the regularity from one level to another. As the noise is white and Gaussian and the decomposition is dyadic and regular, this parameter doubles in value from one scale to another.

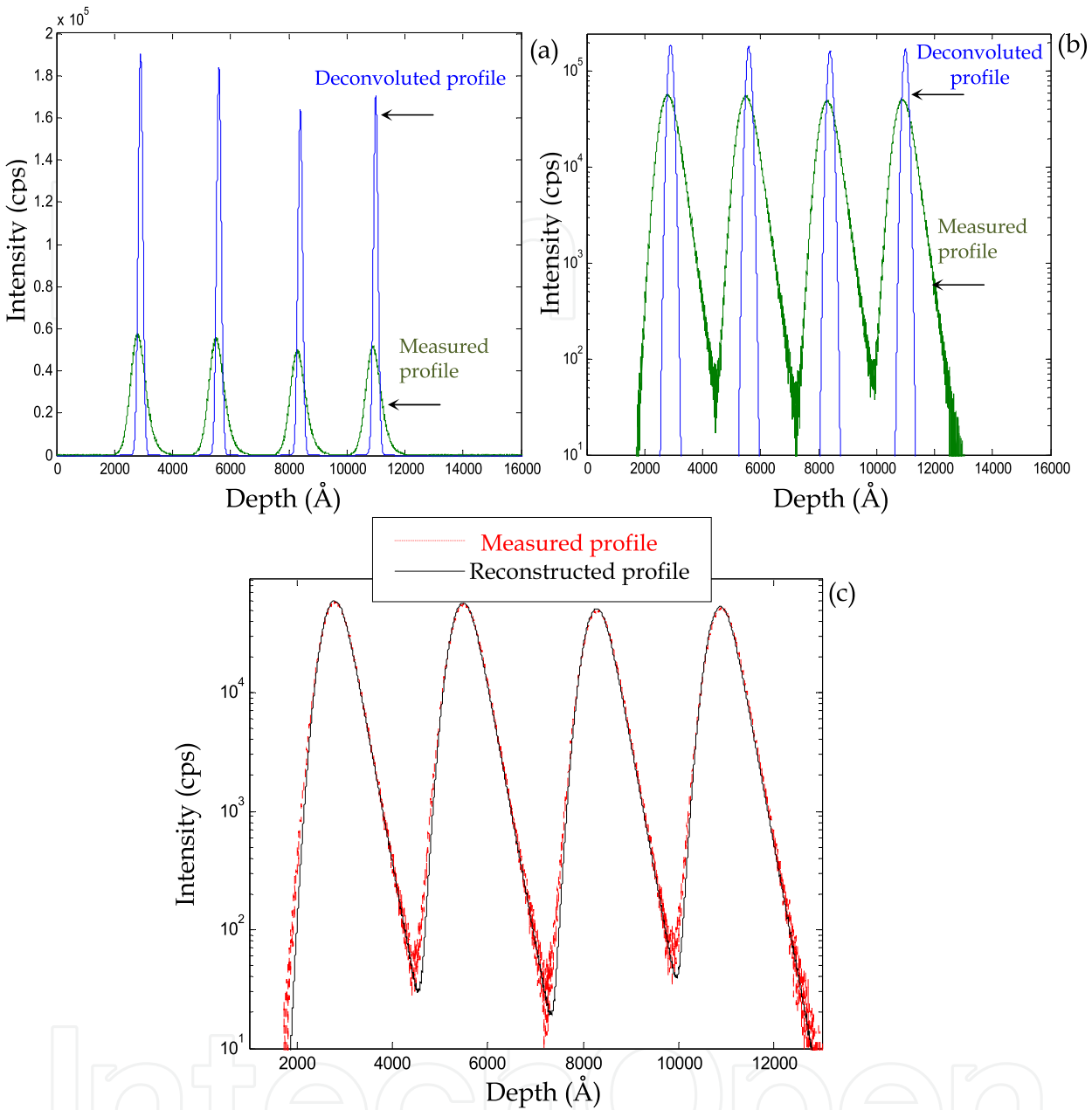


Fig. 9. Results of multiresolution deconvolution of sample MD4 of boron in silicon matrix performed at 8.5 keV/O<sub>2</sub><sup>+</sup>, 38.7°. (a) Linear scale plot. (b) Logarithmic scale plot. (c) Reconstruction of the measured profile from the deconvoluted profile and the DRF. The estimated threshold, obtained using soft universal shrinkage [eq. (17)], is  $\lambda = 55.7831$  cps. The estimated level of noise, using eq. (18), is SNR = 40.9212 dB. The wavelet used was *Sym4* with four vanishing moments.

The regularization parameter of approximation or detail takes different values according to the decomposition level. This enables it to be adapted in a local manner with the treated frequency bands, either low or high frequencies. This adaptation leads to compensate high frequencies contrary to a classical regularization parameter, which treats low frequencies which contain useful signal as high frequencies mainly consisting of noise.

The FWHM of the deconvoluted peaks is equal to 18.9 nm, which corresponds to an improvement in the depth resolution by a factor of 3.1587 [Figs. 9(a) and 9(b)]. The dynamic range is improved by a factor of 2.13 for all peaks. The width of the measured peaks indicates that the  $\delta$ -layers are not real deltas – doping (are not very thin layers); they are closer to Gaussian than delta-layers.

The main advantage of MD is the absence of oscillations which appear in TMMS algorithm results due to the noise effect. Actually, these oscillations appear in most of the classical regularization approaches. The question for the SIMS user is to know whether these small peaks (oscillations) are to be considered as physical features or as deconvolution artifacts. In our opinion, the origin of these oscillations is the presence of strong local concentrations of high frequencies of noise in the signal which cannot be correctly restored by a simple classical regularization.

Figure 9(c) represents the reconstructed depth profile, obtained by convolving the deconvoluted profile with the DRF along with the measured profile. It is in perfect agreement with the measured profile over the entire range of the profile depth. This is a figure of merit of the quality of the deconvolution, and it ensures that the deconvoluted profile is undoubtedly a signal which has produced the measured SIMS profile. A good reconstruction is one of the criteria that confirms the quality of the deconvolution and gives credibility to the deconvoluted profile.

Finally, by using the proposed MD, the SIMS profiles are recovered very satisfactorily. The artifacts, which appear in almost all monoresolution deconvolution schemes, have been corrected. Therefore, this new algorithm can push the limits of SIMS measurements towards the ultimate resolution

## 5. Conclusion

This chapter proposes two robust algorithms for inverse problem to perform deconvolution and particularly restore signals from strongly noised blurred discrete data. These algorithms can be characterized as a regularized wavelet transform. There combine ideas from Tikhonov Miller regularization, wavelet analysis and deconvolution algorithms in order to benefit from the advantages of each. The first algorithm is Tikhonov-Miller deconvolution method, where a priori model of solution, is included. The latter is a denoisy and pre-deconvolved signal obtained firstly by the application of wavelet shrinkage algorithm and after, by the introduction of the obtained denoisy signal in an iterative deconvolution algorithm. The second algorithm is multiresolution deconvolution, based also on Tikhonov-Miller regularization and wavelet transformation. Both local applications of the regularization parameter and shrinking the wavelet coefficients of blurred and estimated solutions at each resolution level in multiresolution deconvolution provide to smoothed results without the risk of generating artifacts related to noise content in the profile. These algorithms were developed and applied to improve the depth resolution of secondary ion mass spectrometry profiles.

The multiscale deconvolution, in particular multiresolution deconvolution (2<sup>nd</sup> algorithm), shows how the denoising of wavelet coefficients plays an important role in the deconvolution procedure. The purpose of this new approach is to adapt the regularization parameter locally according to the treated frequency band. In particular, the proposed method appears to be very well adapted to the case where the signal-to-noise ratio is poor, because in this case the

minimum in the variance of the wavelet coefficients comes out more clearly. Thus, this aspect may be very attractive because it is particularly important to optimize the choice of the regularization parameter, especially at high frequencies. Moreover, the possibility of introducing various *a priori* probabilities at several resolution levels by means of the wavelet analysis has been examined. Indeed, we showed that multiresolution deconvolution can be successfully used for the recovery of data, and hence, for the improvement of depth resolution in SIMS analysis. In particular, deconvolution of delta layers is the most important depth profiling data deconvolution, since it gives not only the shape of the resolution function, but also the optimum data deconvolution conditions for a specific experimental setup.

The comparison between the performance of the proposed algorithms and that of classical monoresolution deconvolution, which is Tikhonov-Miller regularization with model of solution (TMMS), shows that MD results are better than the results of the first proposed algorithm and TMMS algorithm. Because in the classical approaches of the regularization (including our first proposed algorithm), the regularization operator applies in a total way to all bands of the signal. This results in treating low frequencies which contain the useful signal like high frequencies mainly constituted by noise. The result is then an oscillating signal, because the regularization parameter is insufficient to compensate all high frequencies. However, the multiresolution deconvolution (2<sup>nd</sup> algorithm) helps to suppress the influence of instabilities in the measuring system and noise. Particularly this method works very well and does not deform the deconvolution result. It gives smoothed results without the risk of generating a comprehensive mathematical profile with no connection to the real profile, i.e., free- oscillation deconvoluted profiles are obtained. We can say unambiguously that the MD algorithm is more reliable with regards to the quality of the deconvoluted profiles and the compared gains which show the influence of noise on the TMMS results.

The MD can be used in two-dimension applications and generally in many problems in science and engineering involving the recovery of an object of interest from collected data. SIMS depth profiling is just one example thereof. Nevertheless, the major disadvantage of MD is the longer computing time compared to monoresolution deconvolution methods. However, due to the increase of computer power during recent years, this disadvantage has become progressively less important.

## 6. References

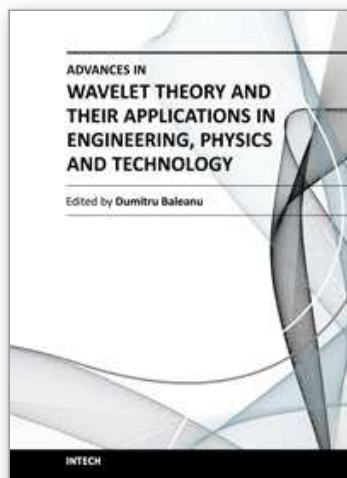
- Allen, P. N., Dowsett, M. G. & Collins, R. (1993). SIMS profile quantification by maximum entropy deconvolution, *Surface and Interface Analysis*, Vol.20, (1993), pp. 696-702, ISSN 1096-9918
- Averbuch, A. & Zheludev, V. (2009). Spline-based deconvolution, *Elsevier, Signal Processing*, Vol.89, (2009), pp. 1782-1797, ISSN 0165-1684
- Barakat, V., Guilpart, B., Goutte, R. & Prost, R. (1997). Model-based Tikhonov-Miller image restoration, *IEEE Explore, Proceedings International conference on Image processing (ICIP '97)*, pp. 310-31, ISBN: 0-8186-8183-7, Washington, DC, USA, October 26- 29, 1997
- Berger, T., Stromberg, J. O. & Eltoft, T. (1999). Adaptive regularized constrained least squares image restoration. *IEEE Transactions on Image Processing*, Vol.8, No9, (1999), pp. 1191-1203, ISSN 1057-7149
- Boulakroune, M., Benatia, D. & Kezai, T. (2009). Improvement of depth resolution in secondary ion mass spectrometry analysis using the multiresolution deconvolution.



- Japanese Journal of applied physics*, Vol.48, No6, (2009), pp. 066503- 1,15, ISSN Online 1347-4065 / Print: 0021-4922
- Boulakroune, M., Eloualkadi, A., Benatia, D., & Kezai, T. (2007) New approach for improvement of secondary ion mass spectrometry profile analysis, *Japanese Journal of applied physics*, Vol.46 No.11, (2007), pp. 7441-7445, ISSN Online: 1347-4065 / Print: 0021-4922
- Boulakroune, M., Slougui, N., Benatia, D. & El Oualkadi, A. (2008). Tikhonov-Miller regularization with a denoisy and deconvolved signal as model of solution for improvement of depth resolution in SIMS analysis, *IEEEExplore, 3<sup>rd</sup> International Conference on Information and Communication Technologies: From Theory to Applications*, pp. 1-6, ISBN 978-1-4244-1751- 3, Damascus, Syria, April 7-11, 2008
- Brianzi, P. (1994). A criterion for the choice of a sampling parameter in the problem of laplace transform inversion. *Journal Inverse Problems*, Vol.10, (1994), pp. 55-61, ISSN 0266- 5611
- Burdeau, J. -L, Goutte, R. & Prost, R. (2000). Joint nonlinéair-quadratic regularization in wavelet based deconvolution schem. *IEEEExplore, Proceedings the 5<sup>th</sup> International conference on signal processing WCCC-ICSP 2000*, Vol.1, pp. 77-80, ISBN 978-1-4577-0538-0, Beijing, China, August 21 - 25, 2000
- Charles, C., Leclerc, G., Louette, P., Rasson, J.-P. & Pireaux, J.-J. (2004). Noise filtering and deconvolution of XPS data by wavelets and Fourier transform, *Surface and Interface Analysis*, Vol.36, (2004), pp. 71-80, ISSN 1096-9918
- Collins, R., Dowsett, M. G. & Allen, A. (1992). Deconvolution of concentration profiles from SIMS data using measured response function, *SIMS proceeding, 8<sup>th</sup> International conference on secondary ion mass spectrometry*, pp. 111-115, ISBN 10 0471930644, Amsterdam, Netherland, September 15-20, 1991
- Connolly, T. J. & Lane, R. G. (1998). Constrained regularization methods for superresolution, *Proceedings IEEE 1998 International conference on image processing ICIP 98*, pp. 727 - 731, ISBN 0-8186-8821-1, Chicago Illinois, California, USA, October 4-7, 1998
- Daubechies, I. (1990). The wavelet transform, time-frequency localization and signal analysis. *IEEE Transaction on Information theory*, Vol.36, No.5, (1990), pp. 961-1005, ISSN 0018-9448
- Donoho, D. L. & Johnstone, I. M. (1994). Ideal spatial Adaptation by wavelet shrinkage, *Biometrika*, Vol.81, No3, (1994), pp. 425-455, ISSN 0006-3444
- Donoho, D. L. & Johnstone, I. M. (1995). Adaptating to unknown smoothness via wavelets shrinkage, *American Statistical Association – Journal*, Vol.90, No.432, (1995), pp. 1200-1224, ISSN 0162-1459
- Dowsett, M. G., Dowlands, G., Allen, P. N., & Barlow, R. D. (1994). An analytic form for the SIMS response function measured from ultra thin impurity layers, *Surface and Interface Analysis* Vol. 21, (1994), pp. 310-315, ISSN 1096-9918
- Essah, W. A. & Delves, L. M. (1988). On the numerical inversion of the Laplace transform). *Journal Inverse Problems*, Vol.4, (1988), pp. 705-724, ISSN 0266-5611
- Fan, J. & Koo, J.-Y. (2002). Wavelet deconvolution, *IEEE Transaction on Information Theory*, Vol.48, No.3, (2002), pp. 734-747, ISSN 0018-9448
- Fares, B., Gautier, B., Dupuy, J. C., Prudon, G., & Holliger, P. (2006). Deconvolution of very low energy SIMS depth profiles, *Applied Surface Science*. Vol. 252, (2006), pp. 6478-6481, ISSN 0169-4332

- Fearn, S. & McPhail, D. S. (2005). High resolution quantitative SIMS analysis of shallow boron implants in silicon using a bevel and image approach. *Applied Surface Science*. Vol.252, No.4, (2005), pp. 893-904, ISSN 0169- 4332
- Fischer, R., Mayer, M., Von der Linden, W. & Dose, V. (1998). Energy resolution enhancement in ion beam experiments with Bayesian probability theory. *Nuclear Instruments and Methods in Physics Research Section B*, Vol.136-138, (1998), pp. 1140-1145, ISSN 0168-583X
- Fujiyama, N., Hasegawa, T., Suda, T., Yamamoto, T., Miyagi, T., Yamada, K., & Karen, A. (2011). A beneficial application of backside SIMS for the depth profiling characterization of implanted silicon, *SIMS Proceedings Papers, Surface & Interface Analysis, The 12th International Symposium on SIMS and Related Techniques Based on Ion-Solid Interactions*, Vol.43, pp. 654–656, ISSN 1096-9918, Seikei University, Tokyo, Japan, June 10-11, 2010
- Garcia-Talavera, M., & Ulicny, B. (2003). A genetic algorithm approach for multiplet deconvolution in g-ray spectra. *Nuclear Instruments and Methods in Physics Research A*, Vol. 512, (2003), pp. 585–594, ISSN 0168-9002
- Gautier, B., Dupuy, J. C., Prost, R. & Prudon, G. (1997). Effectiveness and limits of the deconvolution of SIMS depth profiles of boron in silicon. *Journal of Surface & Interface Analysis*, Vol.25, (1997), 464-477, ISSN 1096-9918
- Gautier, B., Prudon, G., & Dupuy, J. C. (1998). Toward a better reliability in the deconvolution of SIMS depth profiles, *Surface and Interface Analysis*, Vol. 26, (1998), pp. 974-983, ISSN 1096-9918
- Herzel, F., Ehwald, K. -E., Heinemann, B., Kruger, D., Kurps, R., Ropke, W. & Zeindl, H.-P. (1995). Deconvolution of narrow boron SIMS depth profiles in Si and SiGe. *Surface & Interface Analysis*. Vol.23, (1995), pp. 764-770, ISSN 1096-9918
- Iqbal, M. (2003). Deconvolution and regularization for numerical solutions of incorrectly posed problems. *Journal of computational & Applied Mathematics*, Vol.151, (2003), pp. 463- 476, ISSN: 0377-0427
- Jammal, G. & Bijaouib, A. (2004). DeQuant: a flexible multiresolution restoration framework. *Elsevier, Elsevier, Signal Processing*, Vol. 84, (2004), pp. 1049–1069, ISSN: 0165-1684
- Makarov, V. V. (1999). Deconvolution of high dynamic range depth profiling data using the Tikhonov method, *Surf. Interface. Anal.*, Vol. 27, (1999), pp. 801-816, ISSN 1096- 9918
- Mallat, S. G. (1989). A theory for multiresolution signal decomposition: the wavelet representation. *IEEE Transaction on Pattern Analysis and Machine Intelligence*, Vol.11, No7, (1989), pp. 674-692, ISSN: 0162- 8828
- Mancina, G., Prost, R., Prudon, G., Gautier, B., & Dupuy, J.C. (2000). Deconvolution SIMS depth profiles: toward the limits of the resolution by self-deconvolution test, *SIMS Proceedings Papers, the 12th SIMS International Conference*, pp. 497-500 In A. Benninghoven, P. Bertrand, H. N. Migeon, & H. W. Werner, editors, Elsevier, *Proceeding SIMS XII*, ISSN 0169- 4332, Brussels, Belgium, September 5-11, 1999.
- Neelamani, R., Choi, H. & Baraniuk, R. (2004). ForWaRD: Fourier-wavelet regularized deconvolution for ill-conditioned systems, *IEEE Transaction Signal Processing*, Vol.52, No.2, (2004) pp. 418–433, ISSN 1053-587X
- Prost, R. & Goutte, R. (1984). Discrete constrained iterative deconvolution algorithms with optimized rate of convergence. *Elsevier, Signal processing*, Vol.7, No3, pp. 209-230, ISSN 0165-1684

- Rashed, E. A., Ismail, I. A. & Zaki, S. I. (2007). Multiresolution mammogram analysis in multilevel decomposition. *Pattern Recognition Letters*, Vol.28, (2007), pp. 286- 292, ISSN 0167-8655
- Rucka, M., & Wilde, K. (2006). Application of continuous wavelet transform in vibration based damage detection method for beams and plates. *Elsevier, Journal of Sound and Vibration*, Vol.297, No3-5, ( 2006), pp. 536-550, ISSN: 0022-460X
- Seki, S., Tamura, H., Wada, Y., Tsutsui, K., & Ootomoc, S. (2011). Depth profiling of micrometer-order area by mesa-structure fabrication, *SIMS Proceedings Papers, Surf. Interface Anal., The 12th International Symposium on SIMS and Related Techniques Based on Ion-Solid Interactions*, Vol.43, pp. 154-158, ISSN 1096-9918, Seikei University, Tokyo, Japan, June 10-11, 2010
- Shao, L., Liu, J., Wang, C., Ma, K. B., Zhang, J., Chen, J., Tang, D., Patel, S. & Chu, W. -K. (2004). Response Function during Oxygen Sputter Profiling for Deconvolution of Boron Spatial Distribution *Nuclear Instruments and Methods in Physics Research section B*, Vol.219-220, (2004), pp. 303-307, ISSN 0168-583X
- Starck, J-L., Nguyen, M. K. & Murtagh F. (2003). Wavelets and curvelets for image deconvolution: a combined approach. *Elsevier, Signal Processing*, Vol.83, (2003), pp. 2279 - 2283, ISSN 0165-1684
- Stone, M. (1974). Cross-validatory choice and assessment of statistical predictions. *Journal of the Royal Statistical Society: Series B (Statistical Methodology)*, Vol.36, (1974), pp. 111-147, ISSN 1369-7412
- Thompson, A. M., Brown, J. C., Kay, J. W. & Titterington, D. M. (1991). A Study of Methods of Choosing the Smoothing Parameter in Image Restoration by Regularization. *IEEE Transactions on Pattern Analysis and Machine Intelligence*, Vol.13, No.4, (1991), pp. 326-339, ISSN 0162-8828
- Thompson, A. M., Brown, J. C., Kay, J. W. & Titterington, D. M. (1991). A Study of Methods of Choosing the Smoothing Parameter in Image Restoration by Regularization. *IEEE Transactions on Pattern Analysis and Machine Intelligence*, Vol.13, No.4, (1991), pp. 326-339, ISSN 0162-8828
- Tikhonov, A.N. (1963). Solution of incorrectly formulated problems and the regularization method, *Soviet Mathematics Doklady- IAC-CNR*, Vol.4, (1963), pp. 1035-1038, ISSN 0197-6788
- Varah, J. M. (1983). Pitfalls in numerical solutions of linear ill-posed problems. *SIAM Journal on Scientific & Statistical Computing*, Vol.4, No.2, (1983), pp. 164- 76, ISSN 0196-5204
- Weyrich, N. & Warhola, G. T. (1998). Wavelet shrinkage and generalized cross validation for image denoising, *IEEE Transactions on Image Processing*, Vol.7, (1998) pp. 82-90, ISSN 1057-7149
- Yang, M.H. & Goodman, G. G. (2006). Application of deconvolution of boron depth profiling in SiGe heterostructures, *Journal of thin solid films*, Vol.508, (2006), pp. 276-278, ISSN 0040- 6090
- Zheludev, V.A. (1998). Wavelet analysis in spaces of slowly growing splines via integral representation, *Real Analysis Exchange*, Vol.24, (1999), pp. 229-261, ISSN 0147-1937



## **Advances in Wavelet Theory and Their Applications in Engineering, Physics and Technology**

Edited by Dr. Dumitru Baleanu

ISBN 978-953-51-0494-0

Hard cover, 634 pages

**Publisher** InTech

**Published online** 04, April, 2012

**Published in print edition** April, 2012

The use of the wavelet transform to analyze the behaviour of the complex systems from various fields started to be widely recognized and applied successfully during the last few decades. In this book some advances in wavelet theory and their applications in engineering, physics and technology are presented. The applications were carefully selected and grouped in five main sections - Signal Processing, Electrical Systems, Fault Diagnosis and Monitoring, Image Processing and Applications in Engineering. One of the key features of this book is that the wavelet concepts have been described from a point of view that is familiar to researchers from various branches of science and engineering. The content of the book is accessible to a large number of readers.

### **How to reference**

In order to correctly reference this scholarly work, feel free to copy and paste the following:

M'hamed Boulakroune and Djamel Benatia (2012). Multi-Scale Deconvolution of Mass Spectrometry Signals, *Advances in Wavelet Theory and Their Applications in Engineering, Physics and Technology*, Dr. Dumitru Baleanu (Ed.), ISBN: 978-953-51-0494-0, InTech, Available from: <http://www.intechopen.com/books/advances-in-wavelet-theory-and-their-applications-in-engineering-physics-and-technology/multi-scale-deconvolution-of-mass-spectrometry-signals>

**INTECH**  
open science | open minds

### **InTech Europe**

University Campus STeP Ri  
Slavka Krautzeka 83/A  
51000 Rijeka, Croatia  
Phone: +385 (51) 770 447  
Fax: +385 (51) 686 166  
[www.intechopen.com](http://www.intechopen.com)

### **InTech China**

Unit 405, Office Block, Hotel Equatorial Shanghai  
No.65, Yan An Road (West), Shanghai, 200040, China  
中国上海市延安西路65号上海国际贵都大饭店办公楼405单元  
Phone: +86-21-62489820  
Fax: +86-21-62489821

© 2012 The Author(s). Licensee IntechOpen. This is an open access article distributed under the terms of the [Creative Commons Attribution 3.0 License](https://creativecommons.org/licenses/by/3.0/), which permits unrestricted use, distribution, and reproduction in any medium, provided the original work is properly cited.

IntechOpen

IntechOpen